

Ozone UV Spectroscopy. II. Absorption Cross-Sections and Temperature Dependence

J. MALICET, D. DAUMONT, J. CHARBONNIER, C. PARISSÉ,
A. CHAKIR and J. BRION

*Laboratoire de Chimie-Physique, Groupe de Spectrométrie Moléculaire et Atmosphérique
URA D1434, Faculté des Sciences, B.P. 347, 51062 Reims, Cédex, France*

(Received: 21 July 1994; in final form: 2 January 1995)

Abstract. Absolute absorption cross-sections of ozone have been measured at five temperatures (218–295 K) in the UV wavelength region corresponding to the Hartley and Huggins bands (195–345 nm). The aim is to give to the users, a coherent set of data determined under high resolution. A comparison with previous work has been made.

Key words: Ozone, absorption, cross-sections, ultraviolet, temperature dependence.

1. Introduction

The knowledge of the absorption cross-sections of ozone (σ_{O_3}) is of major importance for the study and the monitoring of the atmospheric ozone layer.

In order to have significant results the laboratory measurements need to be carried out in the same conditions of temperature and pressure to those of the stratosphere. Within the framework of a new determination of σ_{O_3} , we first made our measurements at ambient temperature (Daumont *et al.*, 1992), in order to test our apparatus and our method of calculation for the O_3 concentration in the absorption cell. A comparison with the values used in previous work confirms the method we have chosen. Having taken this precaution, we then changed our apparatus in order to make the measurements at very low temperatures, as low as 218 K (Brion *et al.*, 1992, 1993). Experiments have been carried out at 5 temperatures and comparison has been made with the most recent data of Yoshino *et al.* (1988, 1993), Molina and Molina (1986), Bass and Paur (1984) and Cacciani *et al.* (1989).

2. Experimental

The general scheme is that described previously (Malicet *et al.*, 1989; Daumont *et al.*, 1992) (Figure 1). A monochromatic radiation from a spectrometer (Jobin-Yvon THR 1500 or HR 640) is sent through an absorption cell on a photomultiplier (Hamamatsu R 925). A second photomultiplier, located behind a semi-reflecting strip, controls the radiation stability at the exit of the monochromator. Both these

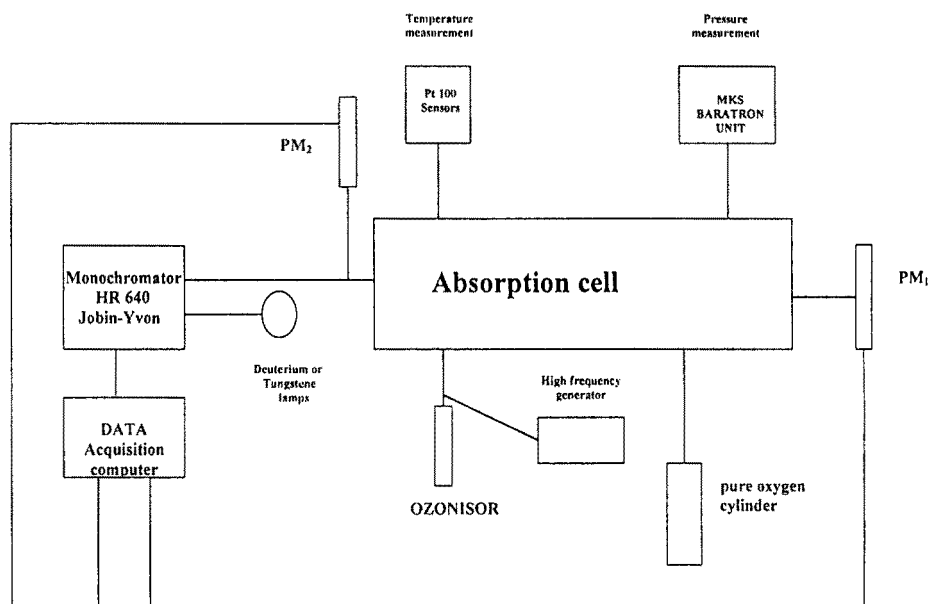


Fig. 1. Experimental scheme.

PM are connected with a computer which permits the acquisition of signal and the treatment of results.

A capacitive manometer (MKS baratron) measures the pressure of gaseous mixture (O_3 , O_2) in the absorption cell all through the experiment. In order to adapt our apparatus to measurements at low temperatures, we used a two-stages cryostat (MATON) enabling us to bring the temperature down to 215 K. Its power is sufficient to maintain a reserve of 200 liters fluorocarbons tank at the working temperature. The cryostat itself is connected to the double-walled absorption cell by a methanol circulation, which plays the role of heat exchanger. In order to limit thermic losses and prevent ambient vapour condensation, vacuum is maintained at each end of the absorption cell, and the whole apparatus is carefully isolated by a 5-cm layer of closed cells foam.

In those conditions, after a lapse of time of about 24 h necessary to reach the thermal stability, the cell temperature can be maintained thus for several weeks. Several high-precision platinum sensors (sensibility 1/50 degree, accuracy 1/10 degree) set along the cell permit a permanent control of the temperature. The difference between measurements made at different parts of the cell does not exceed 0.3 degree and the stability during an experiment lasting 3 h remains below 0.05 degree.

TABLE I. Experimental conditions

Spectral range (nm)	Optical path (m)	Ozone pressure (Torr)	Temperature (K)
195–320	3.285 ± 0.001	1–100	213–273
310–350	99.90 ± 0.05	10–100	213–273
195–335	3.285 ± 0.001	1–600	295
320–350	81.50 ± 0.05	20–200	295
Spectral bandwidth	$\Delta\lambda = 0.01\text{--}0.02$ nm		
Optical density D	$0.5 < D < 2.0$		

This thermal stability is of major importance to maintain our method of partial pressure P_{O_3} calculation because the relation using the total pressure P_T and the oxygene pressure $(P_{O_2})_i$ introduced before the ozonisation:

$$P_{O_3} = 2[(P_{O_2})_i - P_T] \quad (1)$$

is only valid at constant temperature and volume. We can notice that – as we have shown (Daumont *et al.*, 1992) – this relation takes into account the thermal and photochemical decomposition of O_3 in O_2 . In our case, the secondary reactions are negligible, the impurities as H_2O , CO , CO_2 , N_2O having concentrations, measured by FTIR, below to 0.1%.

The O_3 preparation is realized from O_2 ('Air Liquid', N45 purified) with the method described by Griggs (1968). This device permits to obtain a gaseous mixture (O_3 , O_2) with a high concentration of O_3 ($\cong 92\%$). This rate decreases slowly by a few percent during an experiment of a few hours because of the spontaneous ozone decomposition. One notices that this decomposition is slower as the temperature is low.

Nevertheless, in order to take into account this variation and the ozone decomposition, we measure the total pressure P_T and the cell temperature during the spectrum recording. The application of Equation (1) permits us to calculate at any moment the accurate partial pressure, used in the determination of cross-sections.

The experimental conditions of the records are summarized in Table I. At last, in order to minimize errors from different origins, the experimental data are obtained by the average of 10 independent recordings. The uncertainty examination (Table II) shows that those are similar to the ones calculated at ambient temperature. The only difference which appears, is closed to the utilisation of the monochromator (HR 640) slightly less precise in wavelength than the (THR 1500). Indeed, in the spectral regions where the variation $d\sigma/d\lambda$ is important (Huggins bands), we observe a slight increase of the uncertainty. Nevertheless, we can notice that the standard deviation calculated with 10 scans stays underneath total error estimations.

TABLE II. Analysis of errors

Absorbance	1%
Optical path	0.05%
Ozone pressure	0.1%
Temperature	0.02–0.15%
Impurities	< 0.1%
Wavelength	0.005–0.015 nm
Total systematic error	1.3–1.5% (Hartley band) 1.3–3.5% (Huggins band)
Random errors (RMS)	0.3–2.0%
$\lambda < 340$ nm	

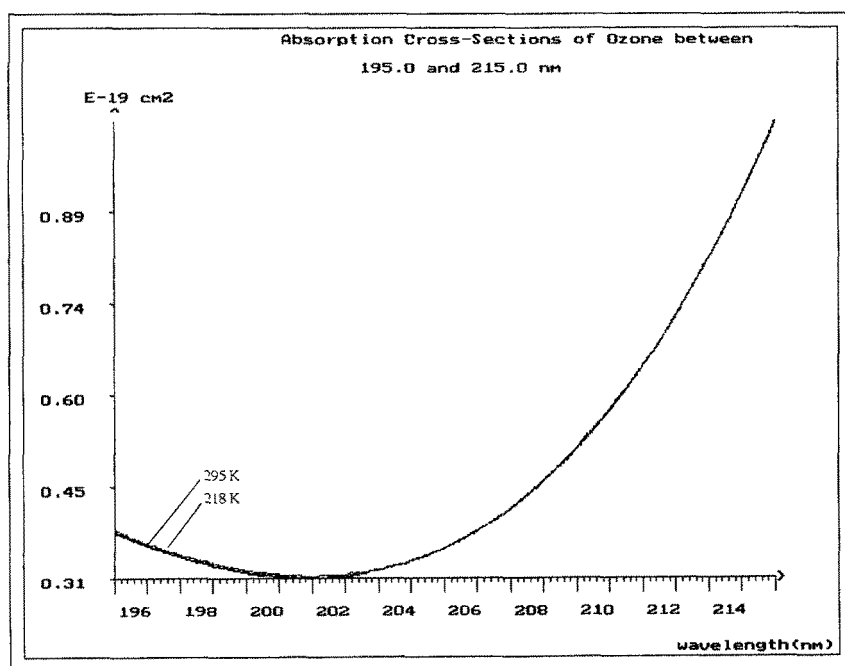


Fig. 2. Ozone cross-sections in the 'optical window' at 210 nm.

3. Results

Our measurements were performed in the 195–345 nm spectral range at 218, 228, 243 and 273 K (Brion *et al.*, 1992, 1993), and so complement our earlier measurements at ambient temperature (295 K).

These measurements cover the whole ozone UV spectrum corresponding to the Hartley (200–310 nm) and the Huggins (310–345 nm) bands (Figures 2 and 3).

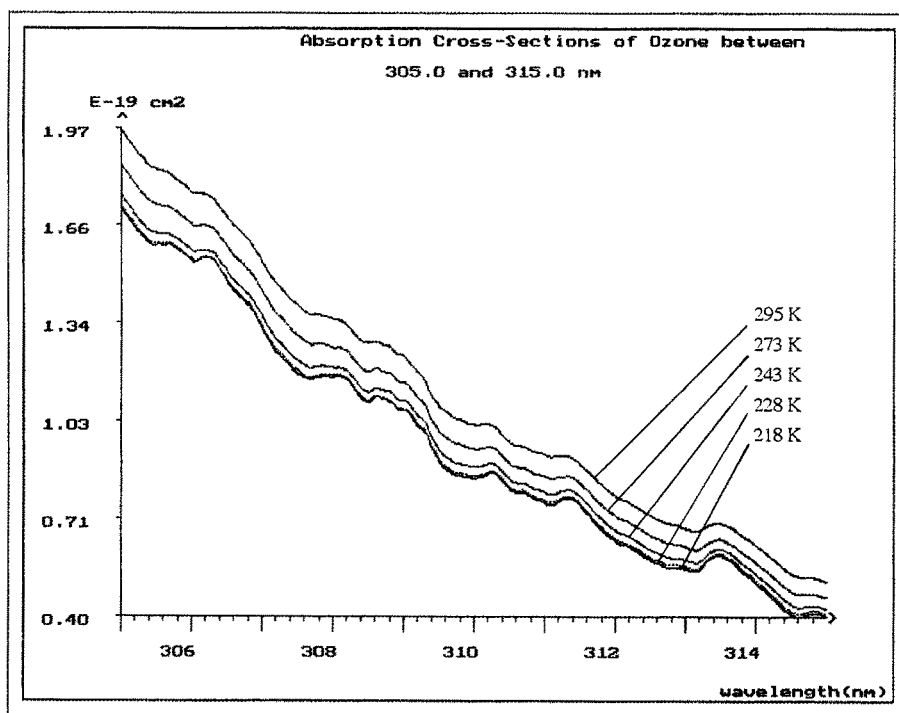


Fig. 3-1.

All these data have been gathered together on a floppy disk, available on request.

3.1. TEMPERATURE EFFECT

Generally, we observe that the effect of temperature on the cross-section values is weak in the Hartley band. Nevertheless, close to the maximum, a rise in the cross-sections is observed when the temperature decreases. However, this variation remains slight: at the mercury wavelength ($\lambda = 253.6$ nm), the cross-sections decrease by 1.0% for a rise in temperature from 218 to 295 K. This variation is comparable with the value (1.15%) determined by the dew-point method previously described (Malicet *et al.*, 1989). It is also in agreement with the variation (0.8%) observed by Molina and Molina (1986) and with the one determined by Atabek *et al.* (1986) by an ab-initio calculation. One can also observe that, at this same wavelength, our results are in very good agreement with the ones determined by Barnes and Mauersberger (1987) for the same temperatures (Table III).

In the 'optical window' centered to 210 nm, we observe no temperature effect, the cross-sections curves at the different temperatures being identical.

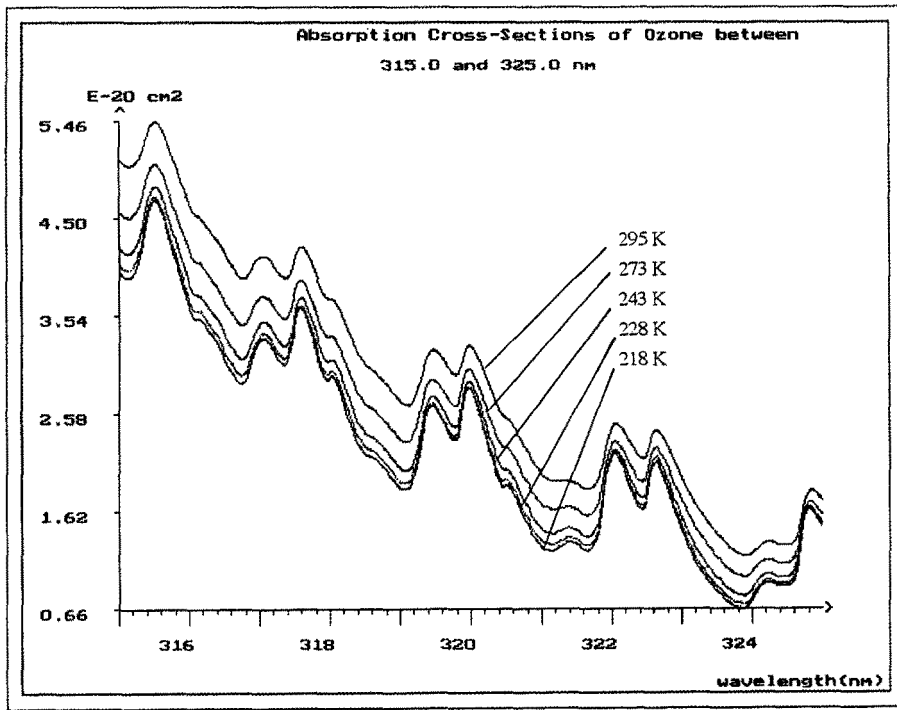


Fig. 3-2.

TABLE III. Absolute cross-sections at 253.65 nm; temperature dependence; comparison

Present work		Barnes and Mauersberger		$\Delta\sigma/\sigma$
T(K)	$\sigma \times 10^{19} \text{ cm}^2$	T(K)	$\sigma \times 10^{19} \text{ cm}^2$	
295	113.05 ± 1.1	297	113.6	-0.48%
273	-	273	114.0	-
243	113.7 ± 1.5	253	114.2	-0.44%
228	113.5 ± 1.5	-	-	-
218	114.1 ± 1.5	221	114.4	-0.26%

On the other hand, in the Huggins bands, the effect of temperature is important and increases progressively as we approach longer wavelengths, where some variation of more than 50% can be observed. In this region, we can notice that, contrary to the situation observed at the maximum of the band, the cross-sections increase with the temperature.

An examination of the curves $\sigma_{\text{O}_3} = f(\lambda)$ at varying temperatures shows a regular increase of the cross-sections in relation to the temperature. To ensure this, we traced the curves $\sigma_{\text{O}_3} = f(\text{temperature})$ at a few particular wavelengths situated

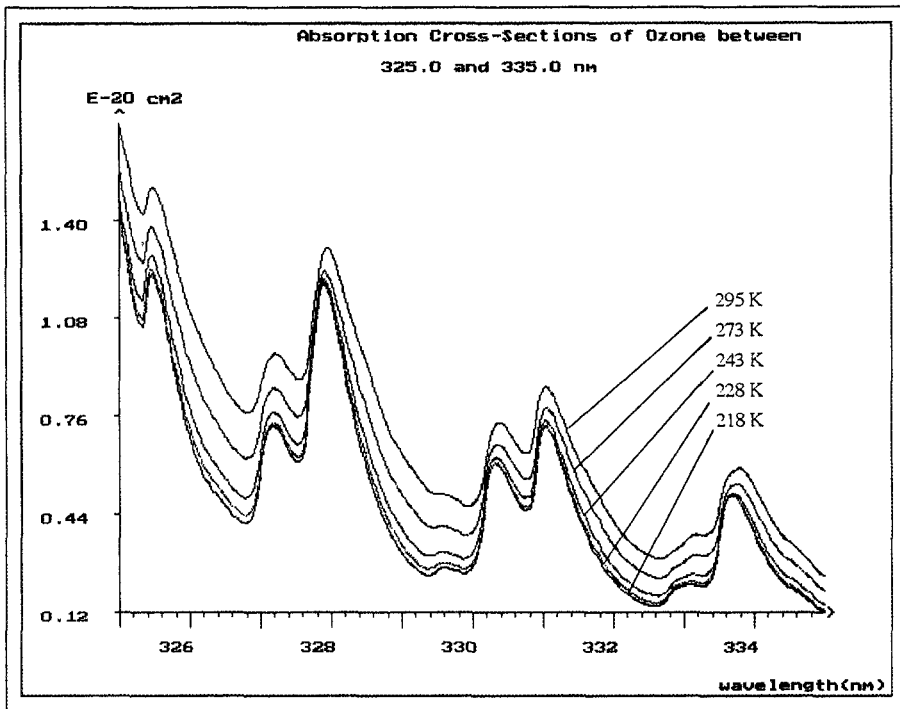


Fig. 3-3.

in the regions where the effect is most significant. The appearance of these curves in the first approximations is linear, within a temperature range between ambient temperature and 228 K. In the case of lower temperatures (218 K), the evolution is less important.

The parametrisation of these curves shows that the latter complies with polynomial formulas of the type:

$$\sigma_{O_3} = C_0 + C_1\theta + C_2\theta^2 \quad (\theta = \text{temperature } ^\circ\text{C})$$

the transition to a 4-coefficient polynomial making no significant improvement in the plot of the curves. These results are in agreement with the conclusion reached by Bass and Paur who also adopt a 3-coefficient equation in order to describe this variation.

Moreover, we can observe that the temperature variation is firmly related to the structure of the bands. A maximum effect is achieved in the zones of weak absorption where the ratio $\sigma_{218}/\sigma_{295}$ is of the order of 0.4 in opposition to the top of the bands where this ratio remains around 0.9.

In addition, this variation in the cross-sections is accompanied by a shift in wavelength of the vibrational structure, the bands moving towards the long wavelength with a rise in temperature. Nevertheless, this effect is relatively weak, the

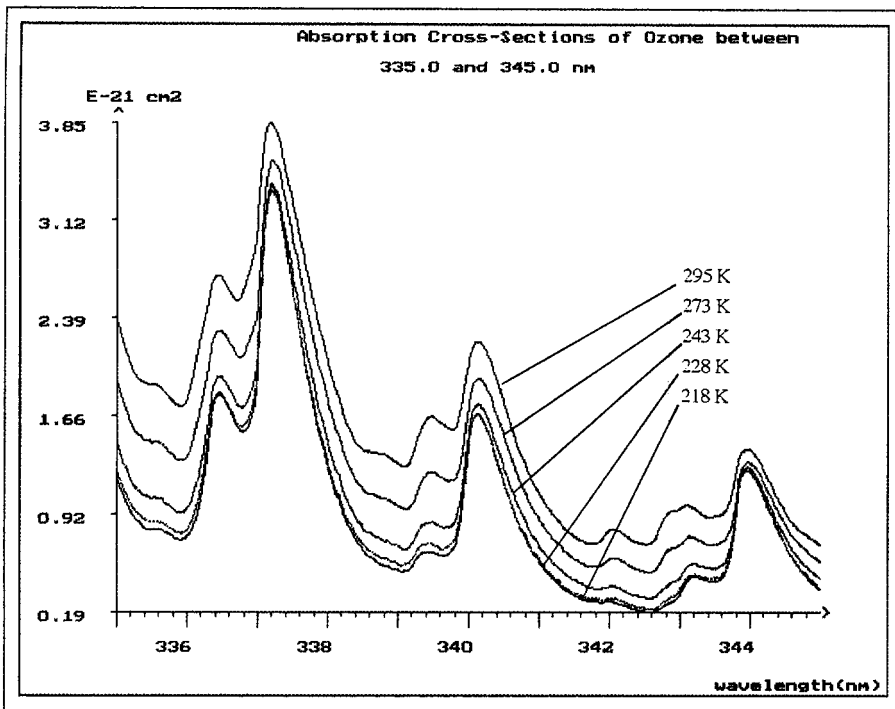


Fig. 3-4.

Fig. 3. Ozone cross-sections in the Huggins bands.

displacements measured on the maxima and minima remain below +0.06 nm for a temperature rise of 218 K to 295 K.

3.2. COMPARISON OF RESULTS

To be sure of the validity of our measurements, we compared them with the most recently published results. However such a comparison is difficult, the measurements having been carried out at different temperatures and in different spectral regions.

At first, the comparison was performed at 228 K with the values determined by Yoshino *et al.* (1988) at 13 fixed wavelengths covering the spectral range 230–345 nm (Table IV). The general agreement is relatively good, the difference between the two series of measures remaining below 1.5% except for 3 values situated between 272 and 289 nm where this difference is about 3%. This agreement between the two series is important, as it shows that the problems linked to measurements at low temperatures have been overcome on both sides.

TABLE IV. Cross-sections values at 228 K (fixed wavelengths)

$\lambda(\text{nm})$	Present work $\sigma \times 10^{19} \text{ cm}^2$	Yoshino <i>et al.</i> $\sigma \times 10^{19} \text{ cm}^2$	$\Delta\sigma/\sigma$
238.20	75.53	75.1	-0.6%
245.76	101.1	100.6	-0.5%
253.65	113.5	115.4	+1.7%
263.58	96.86	96.6	-0.3%
272.09	69.18	67.0	-3.2%
281.32	33.99	33.1	-2.7%
289.36	14.44	14.02	-3.0%
296.73	5.672	5.60	-1.3%
302.15	2.676	2.65	-1.0%
315.13	0.4895	0.486	-0.7%
322.07	0.2180	0.215	-1.4%
334.15	0.03161	0.0311	-1.6%
344.25	0.00984	0.00974	-1.0%

The comparison was next extended to the data of Molina and Molina (195–350 nm), Yoshino *et al.* (1993) (185–254 nm), Bass and Paur (245–340 nm) and Cacciani *et al.* (339–355 nm).

This comparison reveals that the values of Molina and Molina ($T = 226 \text{ K}$) are identical to our own ($\Delta\sigma/\sigma < 1\%$) below 240 nm. This agreement shows that the measurements of Yoshino *et al.* (1993) seem to be too low ($0 < \Delta\sigma/\sigma < 5\%$) in this spectral range. For greater wavelengths, the measures of Molina and Molina are on average greater than our own from 1.5% to 3%.

This good agreement also exists with the values of Bass and Paur in the Hartley band, up to 310 nm, where the differences rarely exceed 1.5% for the 4 temperatures (298, 243, 228 and 218 K). However, in the region of Huggins bands ($\lambda > 310 \text{ nm}$), shifts of +0.05 nm in the vibrational structure of Bass and Paur are visible. This phenomenon having already been observed at ambient temperature is also present at low temperatures, leading to significant differences in the value of the cross-sections. Moreover, an internal comparison of the spectra of Bass and Paur shows that the curve at 218 K presents an additional shift of -0.1 nm in the region 313–318 nm, thus confirming the problems of calibration observed in this latest series of measurements.

The comparison has also been made in the region of 339 and 345 nm with the experimental results of Cacciani *et al.* (1989) (Figure 4). An examination of the curves shows a good agreement in wavelength and in the average values of the cross-sections. Nevertheless we can observe differences in the shape of the bands, our own maxima and minima being greater than those of Cacciani, without it being

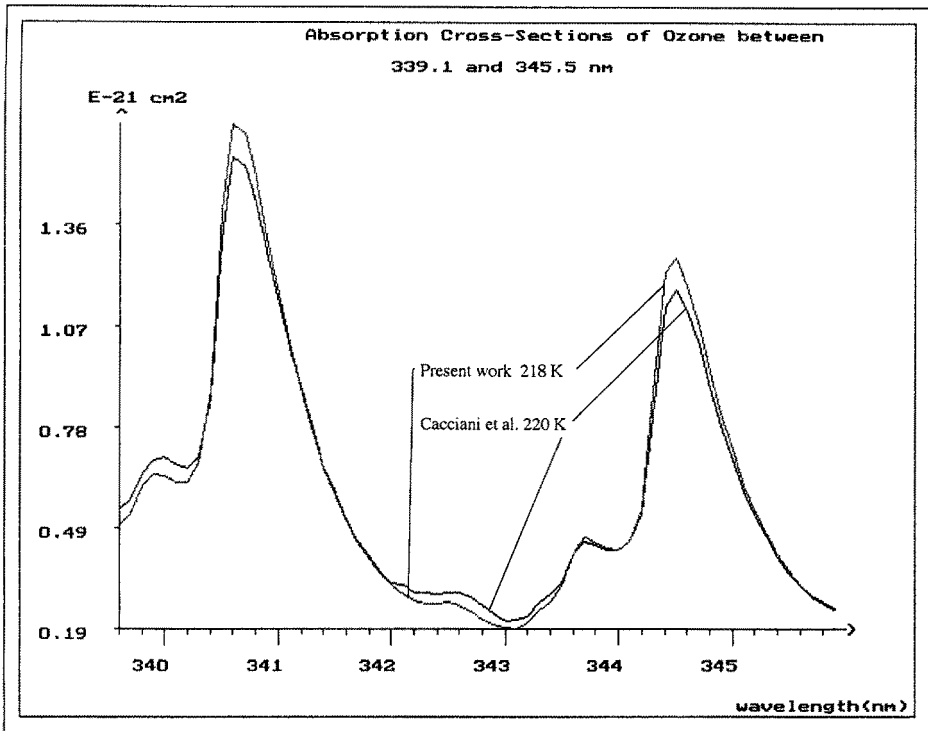


Fig. 4. Absolute cross-sections. Comparison between the data of Cacciani *et al.* and the present work.

possible to explain this difference by different resolutions, the spectral widths used being identical in both cases.

4. Conclusion

The whole values of O_3 cross-sections that we propose, have been determined under high resolution at $T = 295, 273, 243, 228$ and 218 K. They cover the whole spectral region $195\text{--}345$ nm except for the measurements at 273 K which are limited to $300\text{--}345$ nm.

The comparison with the previous and the most recent data shows the validity of our measurements.

These measurements which already form a coherent set of values covering a large spectral range within 5 different temperatures will be in the near future extended to the region of weak absorption in order to meet the new needs of the users.

References

- Atabek, O., Bourgeois, M. T., and Jacon, M., 1986, Three-dimensional analytical model for the photodissociation of symmetric triatomics, Absorption and fluorescence spectra of ozone, *J. Chem. Phys.* **84**, 6699.
- Barnes, J. and Mauersberger, K., 1987, Temperature dependence of the ozone absorption cross-section at the 253.7 nm mercury line, *J. Geophys. Res.* **92**, 14861–14864.
- Bass, A. M. and Paur, R. J., 1984, The ultraviolet cross-sections of ozone, I. Measurements, in C. Zeferos and A. Ghazi (eds.), *Proc. Quadrennial Ozone Symp. Halkidiki, Greece*, Reidel, Dordrecht, pp. 606–616.
- Brion, J., Coquart, B., Daumont, D., Jenouvrier, A., Malicet, J., and Merienne, M. F., 1992, High resolution laboratory absorption cross-sections of O₃ and NO₂, *proc. EUROTRAC Symp.* **92**, SPB Academic Publishing, The Hague, 423–426.
- Brion, J., Chakir, A., Daumont, D., Malicet, J., and Parisse, C., 1993, High-resolution laboratory absorption cross-sections of O₃, temperature effect, *Chem. Phys. Lett.* **213**, 610–612.
- Cacciani, M., Di Sarra, A., Fiocco, G., and Amoruso, A., 1989, Absolute determination of the cross-sections of ozone in the wavelength region 339–355 nm at temperature 220–293 K, *J. Geophys. Res.* **94**, 8485–8490.
- Daumont, D., Brion, J., Charbonnier, J., and Malicet, J., 1992, Ozone UV spectroscopy, I. Absorption cross-sections at room temperature, *J. Atmos. Chem.* **15**, 145–155.
- Griggs, M., 1968, Absorption coefficients of ozone in the ultraviolet and visible regions, *J. Chem. Phys.* **49**, 857–859.
- Malicet, J., Brion, J., and Daumont, D., 1989, Temperature dependence of the absorption cross-section of ozone at 254 nm, *Chem. Phys. Lett.* **158**, 293.
- Molina, L. T. and Molina, M. J., 1986, Absolute absorption cross-sections of ozone in the 185–350 nm wavelength range, *J. Geophys. Res.* **91**, 14501.
- Yoshino, K., Freeman, D. E., Esmond, J. R., and Parkinson, W. H., 1988, Absolute absorption cross-section measurements of ozone in the wavelength region 238–335 nm and the temperature dependence, *Planet. Space Sci.* **36**, 395–398.
- Yoshino, K., Esmond, J. R., Freeman, D. E., and Parkinson, W. H., 1993, Measurements of absolute cross-sections of ozone in the 185 to 254 nm wavelength region and the temperature dependence, *J. Geophys. Res.* **98**, 5205–5211.